AtMAP70-5, a divergent member of the MAP70 family of microtubule-associated proteins, is required for anisotropic cell growth in *Arabidopsis*

Andrey V. Korolev*, Henrik Buschmann, John H. Doonan and Clive W. Lloyd

Department of Cell and Developmental Biology, John Innes Centre, Norwich, NR4 7UH, UK

*Author for correspondence (e-mail: andrey.korolev@bbsrc.ac.uk)

Accepted 2 May 2007
Journal of Cell Science 120, 2241-2247 Published by The Company of Biologists 2007
doi:10.1242/jcs.007393

Summary

AtMAP70-5 is the most divergent of a recently described multigene family of plant-specific microtubule-associated proteins (MAPs). It is significantly smaller than other members and has several isoform-specific sequence features. To confirm that this protein still functions as a MAP we show that it directly binds microtubules in vitro and decorates microtubules in vivo. When added to tubulin polymerization assays, AtMAP70-5 increases the length distribution profile of microtubules indicating that it stabilizes microtubule dynamics. The overexpressed fusion protein perturbs cell polarity in cell suspensions by inducing extra poles for growth. Similarly, in *Arabidopsis* plants the overexpression of AtMAP70-5 causes epidermal cells to swell; it also stunts growth and induces right-handed organ twisting. RNAi-mediated downregulation of AtMAP70-5 results in reduced inflorescence stem length and diameter and individual cells are inhibited in their capacity for expansion. These observations suggest that the control over AtMAP70-5 expression levels is important in order to maintain axial polarity and to ensure regular extension of plant organs.

Supplementary material available online at
http://jcs.biologists.org/cgi/content/full/120/13/2241/DC1

Key words: MAP70, Microtubule-associated protein, Helical growth, *Arabidopsis thaliana*

Introduction

The ability of plants to project into the environment depends upon the ability of their cells to undergo anisotropic expansion. The direction in which cells expand is believed to be regulated according to the way that cellulose microfibrils are wrapped around the cell (Ehrhardt and Shaw, 2006). In turn, there is evidence that the alignment of cellulose is influenced, at least in part, by underlying cytoplasmic microtubules. For example, recent studies have shown that particles labelled for one of the cellulose synthesizing enzymes, AtCESA6, can move along paths provided by cortical microtubules (Paredez et al., 2006).

Drug studies and mutants have emphasized the involvement of cortical microtubules in anisotropic cell expansion. In *Arabidopsis* mutants such as *fass* (also known as *ton2*), the cortical microtubule array is severely compromised and cell anisotropy is lost, resulting in bloated cells and stunted organs (Torres-Ruiz and Jurgens, 1994; Traas et al., 1995). Milder phenotypes are shown by so-called helical growth mutants in which defective cell elongation produces left-handed or right-handed (depending on the allele) organ twisting. In these mutants, organ twisting is assumed to be the direct result of helically arranged microtubules found underneath the plasma membrane of elongating cells (Furutani et al., 2000). Identification of the genes involved in helical growth has revealed microtubule-associated proteins from plants (Buschmann et al., 2004; Perrin et al., 2007; Whittington et al., 2001) and mis-sense mutations in α-tubulin (Thitamadee et al., 2002). These results underline the existence of a chiral component within the machinery controlling cell elongation.

Growing evidence supports the importance of microtubule dynamics in cortical microtubule organization and in helical growth. Cortical microtubules are constantly being remodelled by a hybrid treadmilling mechanism in which the plus end grows faster than the minus end shrinks (Shaw et al., 2003). Encounters between microtubules within the array may lead to catastrophic depolymerization or to ‘zippering’, where microtubules come to lie alongside each other (Dixit and Cyr, 2004). Lateral interaction between microtubules may be facilitated by cross-linking proteins such as members of the MAP65 family, believed to support uniform array orientation and microtubule stabilization (Chan et al., 1999; Smertenko et al., 2000). Several examples demonstrate that microtubule destabilization leads to left-handed helical growth in *Arabidopsis*. Mutation of the microtubule-associated protein MOR1, which is related to the vertebrate XMAP215 family involved in the regulation of microtubule dynamics, produces short cortical microtubules and left-handed root growth (Whittington et al., 2001). Similarly, *lefty1* and *lefty2* mis-sense mutations of α-tubulin result in cortical array destabilization and left-handed root twisting (Abe et al., 2004). By contrast, microtubule stabilization may lead to right-handed helical growth. This was suggested by results obtained for *Arabidopsis* plants expressing N-terminally tagged α-tubulin. Microtubules of these plants showed decreased shrinkage rates and higher rescue frequencies indicative of microtubule stabilization (Abe and Hashimoto, 2005). Right-handed growth was also observed

in the *spiral1* (also known as *sku6*) mutant. SPIRAL1/SKU6 is a microtubule-interacting protein that binds to the plus ends of microtubules and has been suggested to regulate microtubule dynamics (Nakajima et al., 2004; Sedbrook et al., 2004).

In a search for novel plant MAPs, we undertook a proteomic survey of proteins binding microtubules in *Arabidopsis* homogenates (Korolev et al., 2005). In this way a range of proteins was identified, including a high molecular mass MAP, AIR9 (Buschmann et al., 2006), and MAP70 (Korolev et al., 2005). As a GFP fusion, AtMAP70-1 constitutively labelled all four microtubule arrays in vivo and is the founder member of a five-member family of genes in *Arabidopsis* (Korolev et al., 2005). Within this multi-gene family, AtMAP70-1, -2, -3 and -4 share 70-80% identity and approximate 70 kDa molecular mass. However, AtMAP70-5 is different in terms of its smaller size (58 kDa) and in the fact that it shares only 47% sequence identity. This suggested that the differences could be targeted to explore the functionality of AtMAP70-5 in planta. The in vitro properties of AtMAP70-5 indicate that it affects microtubule dynamics and overexpression and gene silencing in *Arabidopsis* plants suggest a role in anisotropic cell expansion and organ growth.

Results

AtMAP70-5 is the most divergent member of the AtMAP70 family

The computational analysis of the AtMAP70-5 deduced amino acid sequence revealed that this isoform is the most divergent member of the *Arabidopsis* MAP70 family. Unlike the other four members, which range between 67.3 and 69.8 kDa, AtMAP70-5 encodes a polypeptide of 513 amino acids with a significantly lower molecular mass of 58.5 kDa. AtMAP70-5 shows no more than 47% amino acid identity to other members of the family. The difference from other AtMAP70 sequences is most pronounced in a spacer connecting the N-terminal and central coiled-coil domains with the C-terminal coiled-coil domain. In AtMAP70-1 this spacer was implicated in microtubule binding (Korolev et al., 2005). Furthermore, AtMAP70-5 is missing an N-terminal extension (about 60 amino acids in size) seen in the other members. The rice genome contains several MAP70 homologues. In the phylogenetic tree, a sequence from rice (Os12g0640900) groups with the *Arabidopsis* MAP70-5 homologue and not with the other *Arabidopsis* or rice MAP70 sequences (Korolev et al., 2005), indicating an early functional diversification of MAP70-5 proteins.

AtMAP70-5 contains a pentapeptide motif, KLEEK, which is also found in the WVD2 family of MAPs (Perrin et al., 2007). In the N-terminal region of AtMAP70-5 this motif is imperfectly repeated at least twice (Fig. 1A). In the WVD2 family of proteins the invariant KLEEK motif is part of a larger 'KLEEK domain' – a stretch of approximately 90 highly conserved amino acids. However, in AtMAP70-5 similarity to the 'KLEEK domain' is limited to a stretch of approximately 30 residues (Fig. 1B). In both classes of MAP the KLEEK motif is part of a predicted coiled-coil region. In AtMAP70-5 and WVD2 the KLEEK motif shows the same position within the heptad repeat of the predicted coiled-coil (Fig. 1B).

AtMAP70-5 interacts with microtubules in vitro

As the most divergent of the MAP70 family it was necessary to investigate whether AtMAP70-5 does behave as a

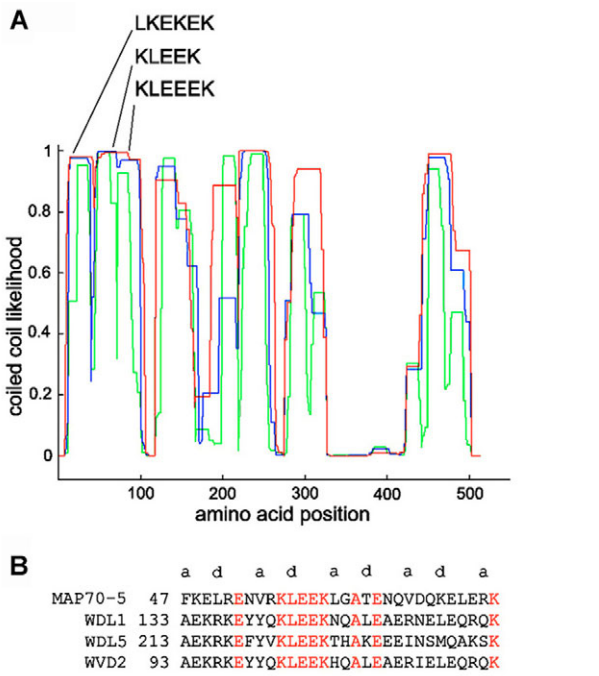

Fig. 1. Computational analysis of the AtMAP70-5 protein. (A) Prediction of coiled-coil domains by the COIL program (Lupas, 1996). Shown is an output based on parameters producing the highest stringency. The relative positions of the KLEEK motif and its imperfect repeats are indicated. The colour of the graphs indicates the window size used in the scan (red 28, blue 21 and green 14 amino acids window). (B) The KLEEK motif and neighbouring amino acids of AtMAP70-5 and the WAVE-DAMPENED 2 (WVD2) family. Identical amino acid positions are in red. The heptad pattern of the predicted coiled-coils (presented by amino acid positions a and d) is shown in the first line.

microtubule-associated protein. The founding member of the family, AtMAP70-1, was previously shown to co-sediment with microtubules polymerized with Taxol out of an homogenate of *Arabidopsis* suspension cells (Korolev et al., 2005). Here, AtMAP70-5 and AtMAP70-1 (as a control) were bacterially expressed as 6xHis fusions (Fig. 2 lanes 1 and 6, respectively) and purified on a metal affinity column. Both were found to interact with pre-assembled microtubules that sedimented through the sucrose barrier (Fig. 2 lanes 2 and 8). AtMAP70-5 (Fig. 2 lane 3) was virtually undetectable in the supernatant and only a relatively minor amount of AtMAP70-1 remained in the supernatant (Fig. 2 lane 9). In the absence of pre-assembled microtubules, neither protein was able to form a pellet (Fig. 2 lanes 4 and 10) and remained in the supernatant (Fig. 2 lanes 5 and 11).

AtMAP70-5 changes the size distribution of microtubules in vitro

To examine the effect of AtMAP70-5 on microtubule dynamics, the bacterially expressed 6xHis-AtMAP70-5 was tested in in vitro microtubule polymerisation assays. AtMAP70-5 in a range of concentrations from 1-10 μg/ml was not found to alter the critical concentration (C_{crit}) for tubulin, which remained in a range of 0.5-0.6 μg/ml. However, when AtMAP70-5 was added after tubulin had been allowed to undergo self-assembly, the number of microtubules per imaged field decreased from

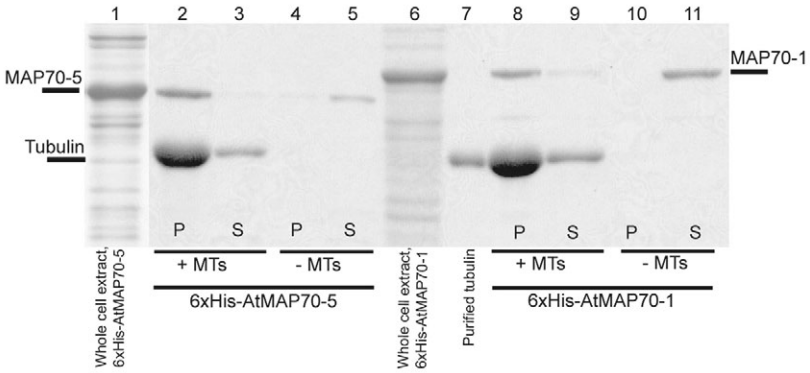

Fig. 2. Recombinant AtMAP70-1 and AtMAP70-5 co-sediment with pre-assembled microtubules in vitro. Lanes 1 and 6: extracts of *E. coli* cells expressing 6xHis-AtMAP70-5 and 6xHis-AtMAP70-1, respectively; concentrations of the purified proteins were estimated as 50 μg/ml for 6xHis:AtMAP70-1 and 10 μg/ml for 6xHis:AtMAP70-5 using SDS-PAGE and BSA standards (not shown). Lane 7: purified tubulin used to form microtubules, but before assembly with Taxol. Lanes 2-5: co-sedimentation of 6xHis-AtMAP70-5 with pre-assembled microtubules. Lanes 8-11: co-sedimentation of 6xHis-AtMAP70-1 with pre-assembled microtubules; P, pellets (lanes 2, 4, 8 and 10); S, supernatants (lanes 3, 5, 9 and 11); + Mts, pre-assembled microtubules added to the reaction mixture (lanes 2, 3, 8 and 9); – Mts, no pre-assembled microtubules added (lanes 4, 5, 10 and 11).

295±39 to 73±11. This was accompanied by an increase in the length of microtubules (Fig. 3B) compared to the MAP-free control (Fig. 3A). In the control, microtubule length peaked at 3-4 μm (mean 4.4±1.0 μm). By contrast, addition of AtMAP70-5 (Fig. 3B) resulted in an approximate doubling of the length of microtubules (max. 7-8 μm; mean length 8.6±2.5 μm).

AtMAP70-5 decorates microtubules in vivo and alters cell polarity

To locate AtMAP70-5 in living cells, we generated stably transformed transgenic tobacco BY-2 suspension cells expressing the protein as an N-terminal GFP fusion. The fusion protein labelled cortical microtubules (Fig. 4D-G) and all mitotic arrays (data not shown). Although the cortical microtubules were labelled in a linear fashion the decoration was more diffuse or punctate (Fig. 4D,E) than seen with GFP-TUA6 or GFP-AtMAP70-1 (Fig. 4B and C, respectively). Out of 1000 BY-2 cells expressing detectable GFP-AtMAP70-5, 25.8% were multipolar (usually tripolar; Fig. 4E). Such abnormalities were rare in cells expressing GFP-TUA6 (Fig. 4B) and GFP-AtMAP70-1 (Fig. 4C), where they occurred at a frequency (1.63% and 1.56%, respectively) little different to untransformed cells (0.60%; Fig. 4A). Similar punctate microtubule labelling was found in roots of GFP-AtMAP70-5 transformed plants (Fig. 4F,G).

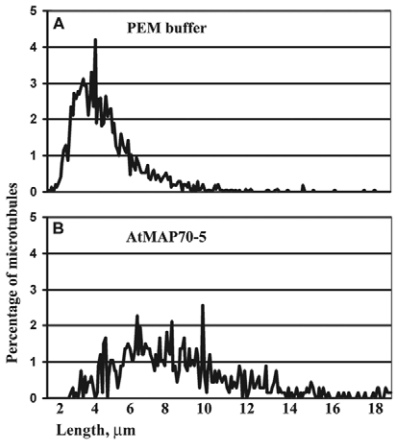

Fig. 3. The effect of added AtMAP70-5 on the length of pre-assembled microtubules in vitro. Tubulin was polymerized before either PME buffer (A) or AtMAP70-5 (B) was added. Addition of AtMAP70-5 shifts the size distribution towards longer microtubules.

The expression level of AtMAP70-5 influences the direction of growth

To investigate the role of AtMAP70-5 in planta we generated transgenic *Arabidopsis* plants containing either *35S::GFP-AtMAP70-5* or untagged *35S::AtMAP70-5* constructs. Of the obtained lines, 17 out of 32 showed a striking twisting of organs (Fig. 5B,D) and we found that the twisting phenotype was always correlated with elevated levels of *AtMAP70-5* mRNA (Fig. 5I) and AtMAP70-5 protein (Fig. 5K). Roots, hypocotyls and petioles of AtMAP70-5 overexpressors showed right-handed twisting accompanied by right-handed rotation of cell files (Fig. 5B,D,F). The majority of the root epidermal cells

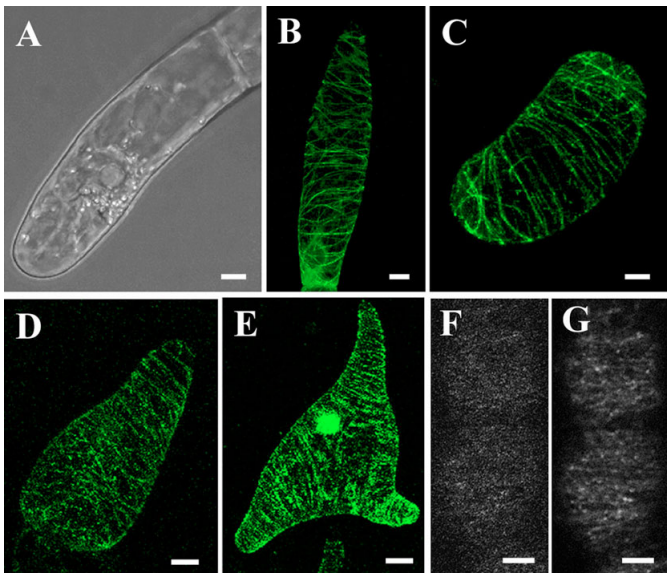

Fig. 4. Labelling patterns of cortical microtubules in tobacco BY-2 cells. (A-E) Untransformed cell (A) and cells stably transformed with GFP-TUA6 (B), GFP-AtMAP70-1 (C) and GFP-AtMAP70-5 (D,E). One in four cells expressing GFP-AtMAP70-5 had additional poles of growth (E). (F,G) Root epidermal cells of GFP-AtMAP70-5-overexpressing *Arabidopsis* plant show punctate labelling (F); when displayed as a time-lapse projection these punctae can be seen to resolve as linear cortical microtubules (G). Bars, 10 μm.

were short and swollen (Fig. 5F), indicating that growth anisotropy was compromised, as had been found for the transgenic cell suspensions (Fig. 4E). To investigate whether overexpression of AtMAP70-5 was affecting the orientation of cortical microtubules we labelled epidermal root cells with anti-tubulin antibodies for immunofluorescence. Whereas root cells from wild-type plants contained mainly transverse microtubule arrays, AtMAP70-5 overexpressors displayed shallow left-handed microtubule helices (Fig. 5G and H, respectively).

Inflorescence stems of overexpressing soil-grown plants were almost twice as short as untransformed wild-type plants (Fig. 6B and Table 1) without a significant effect on the stem diameter (Table 1). In multiple independent lines the siliques of the overexpressing plants were shorter than those of wild type (1.09±0.11 cm versus 1.36±0.11 cm, respectively). This could be associated with decreased fertility since the overexpressors produced fewer seeds (data not shown). Overexpressors also showed right-handed twisting of stems (Fig. 6B).

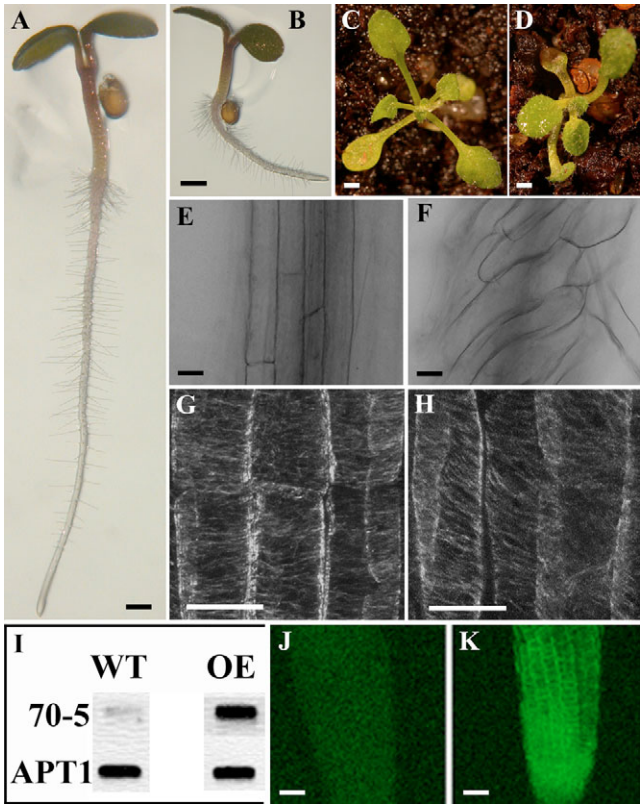

Fig. 5. Overexpression of *GFP-AtMAP70-5* induces right-handed helical growth. (A,B) Three-day-old seedlings grown vertically on a Phytagel plate; A, wild type, B, GFP-AtMAP70-5 overexpressor showing right-twisting root. (C,D) Two-week-old plants; (C) wild type, (D) GFP-AtMAP70-5 overexpressor, illustrating right-twisting petioles. (E,F) Root epidermal cells from plants as in A and B, illustrating right-twisting epidermal files in the overexpressor (F). (G,H) Microtubules in root epidermal cells of the early elongation zone showing shallow left-handed microtubule helices in the overexpressor (H). (I) Semi-quantitative RT-PCR with AtMAP70-5 (70-5)- and APT1-specific primers shows that the twisted phenotype corresponds to high level of AtMAP70-5 expression. (J,K) Root growth under low levels of GFP-AtMAP70-5 expression (J) is straight but with higher expression levels the cell files twist (K). Bars, 1 mm (A-D); 30 μm (E-H); 100 μm (J,K).

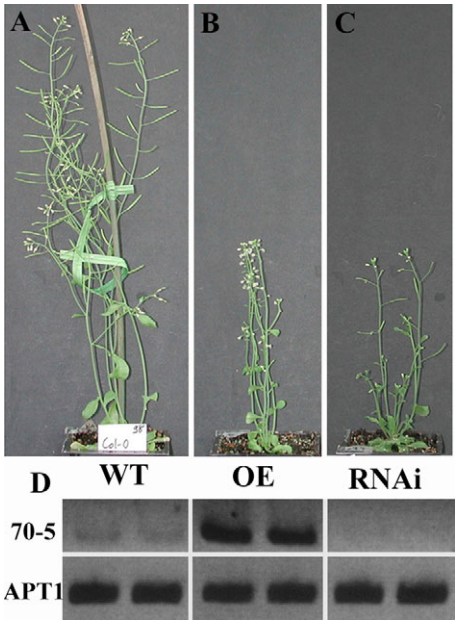

Fig. 6. Overexpression and RNAi knockdown of *AtMAP70-5* generate stunted inflorescence stems. (A-C) Six-week-old wild-type (WT), overexpressor (OE) and RNAi-transformed *Arabidopsis* plants, respectively. (D) RT-PCR (25 cycles) based on total RNA from inflorescence stems (shown for two individuals each) using *AtMAP70-5* (70-5) and *APT1*-specific primers.

To determine whether this reduction in the size of overexpressing plants correlated with a reduction in cell size, we measured epidermal and cortical cells. We found that epidermal and cortical cells in inflorescence stems of overexpressors were significantly shorter than in wild-type plants (Table 1).

Depleting AtMAP70-5 by RNAi disturbs plant development

To investigate the effects of AtMAP70-5 downregulation, we examined two available t-DNA insertion lines but no obvious phenotypes were detected (not shown). Therefore we produced *AtMAP70-5* RNAi plant lines. Five independent lines were generated and examined. At the seedling stage we were unable to detect any obvious phenotype in RNAi plants. However, when 1-week-old seedlings were transferred to soil and grown until flowering each line produced progeny with varying degrees of dwarfism (Fig. 6C). RT-PCR confirmed that *AtMAP70-5* was expressed in inflorescence stems, but was significantly diminished in RNAi dwarf plants (Fig. 6D). To

Table 1. Analysis of AtMAP70-5 overexpressors and RNAi plants

	WT	Overexpressors	RNAi
Plant height (cm)	25±2	14±3**	15±4**
Stem diameter (mm)	0.74+0.08	0.77±0.06 (ns)	0.63±0.08*
Cell length			
Epidermal (μm)	211±49	173±44*	161±41*
Cortical (μm)	31±9	24±7*	21±8*

*Significant at >95% and **significant at >99% confidence interval and ns, not significant, using Student's *t*-test.

check that the RNAi suppression was limited to *AtMAP70-5*, we extracted mRNA from stems of RNAi plants and performed RT-PCR using pairs of primers specific for the different *MAP70* genes (see Fig. S1 in supplementary material). This established that *AtMAP70-5* was the only member of the *MAP70* gene family whose expression was reduced in *AtMAP70-5*-RNAi plants, thereby confirming the specificity of the RNAi construct (see Fig. S1 in supplementary material).

These results also confirmed a Genevestigator (https://www.genevestigator.ethz.ch) meta-analysis (see Fig. S2 in supplementary material), which had suggested that the *AtMAP70-5* gene was expressed in wild-type *Arabidopsis* stems at higher levels than the other four *MAP70* genes. This analysis further indicated that *AtMAP70-5* was the major *MAP70* gene expressed in the stem and in the root hair zone, whereas expression was very low in seedlings, leaves and flowers.

Quantitative analysis of the RNAi dwarfs demonstrated that these plants were significantly shorter (average height 15±4 cm) than wild-type plants (25±3 cm) and their stems were also narrower (0.63±0.08 mm diameter) than those of the wild type (0.74±0.08 mm) (Table 1). Next, we measured the lengths of epidermal and cortical cells in the RNAi dwarfs and found that they were also significantly shorter than in the wild type (161±41 μm versus 211±49 μm and 21±8 μm versus 31±9 μm, respectively) (Table 1). However, in contrast to the AtMAP70-5 overexpressors, we found that the RNAi plants had no swollen cells and did not twist. The number of vascular bundles and the number of cells in stem pith was reduced in the RNAi dwarfs but not in the overexpressors (not shown). These differences suggests that the reduction in the length of inflorescence stems seen in both RNAi and overexpressing plants is achieved in different ways.

Discussion

AtMAP70-5 is a plant-specific MAP

We were prompted to investigate AtMAP70-5 since it appears to have diverged from the group formed by the other four AtMAP70 family members. It is significantly smaller because it is missing the N-terminal extension, it contains the KLEEK pentapeptide motif and the lower overall sequence similarity underlines its difference from the other members.

The fact that we did not detect AtMAP70-5 in our screen for novel MAPs on endogenous Taxol-stabilised microtubules (Korolev et al., 2005) may be attributable to the low expression of the protein in suspension cells (Fig. S2 in supplementary material). However, since not all members of multigenic families of plant MAPs (e.g. the AtMAP65 family) necessarily segregate with microtubules (Mao et al., 2005; Van Damme et al., 2004a; Van Damme et al., 2004b) it was important to confirm that this outlying member of the MAP70 family actually behaves as a MAP. This was tested by adding bacterially expressed protein to purified microtubules in co-sedimentation assays, showing that the protein does directly bind microtubules. In addition, expressed as a GFP fusion, both transiently in *Arabidopsis* suspension cells and as stable tobacco BY-2 cell lines, AtMAP70-5 uniformly decorates cortical microtubules.

To gain further insight into the interaction between microtubules and AtMAP70-5, the bacterially expressed protein was added to tubulin and allowed to self-assemble in vitro. Recombinant AtMAP70-5 in molar ratios up to 10 AtMAP70-5 to 1 tubulin were found to have no effect on lowering the C_{crit} for tubulin assembly but the protein did have a significant effect on the length of already assembled microtubules. But not all MAPs do lower the C_{crit} for tubulin as was shown for biochemically purified carrot MAP65 in vitro (Chan et al., 1996) and for bacterially expressed AtMAP65-1 (Smertenko et al., 2004). Both cross-bridged microtubules but neither of them stimulated the polymerization of tubulin.

In the presence of AtMAP70-5, the size distribution was shifted towards increasing microtubule length as compared to the buffer-only control; there were fewer short microtubules and increased numbers of microtubules longer than 10 μm. This suggests that AtMAP70-5 is shifting the steady-state for microtubule assembly, increasing the on-rate relative to the off-rate. This could be due to an increased polymerization rate, increased rescue, and/or inhibition of catastrophe. Whatever the molecular mechanism, the observed shift in the microtubule size distribution indicates that AtMAP70-5 has a stabilizing effect on microtubule assembly.

The effects of increasing and decreasing levels of AtMAP70-5

In stable tobacco BY-2 lines overexpressing GFP-AtMAP70-5 the cell shape was frequently altered, with one in four interphase cells becoming multipolar. Multipolar cells were observed in *TPLATE* RNAi tobacco BY-2 lines, where it was attributed to possible mis-targeting of cell wall-modifying factors due to reduced activity of the TPLATE protein (Van Damme et al., 2006). BY-2 cells normally grow in cylindrical chains but the multipolar cells were generally single and swollen. In our GFP-AtMAP70-5-overexpressing lines we found that such tripolar (or occasionally tetrapolar) cells contained cortical microtubules that were perpendicular to each axis of expansion. This perturbation of cell polarity observed in stable cell suspensions was reflected in epidermal cells of *Arabidopsis* plants overexpressing AtMAP70-5. Fig. 5F shows that root epidermal cells were shorter and swollen. The overall morphology of the mutant plants was also severely affected since growth was stunted and various organs (including roots, hypocotyls, petioles and inflorescence stems) showed right-handed twisted growth. Right-handed helical growth is seen in knockout mutants of other microtubule-related proteins such as SPIRAL1 (SPR1) (Furutani et al., 2000). SPR1 is a small (12 kDa) protein that locates to the faster-growing plus ends of microtubules and disappears when the microtubule shrinks, suggesting a role in promoting polymerization and/or discouraging pause or depolymerization (catastrophe) at the plus ends (Sedbrook et al., 2004). However, in time-lapse movies, we found no evidence for the preferential localization of GFP-AtMAP70-5 to either end, with fluorescence distributed along the length of microtubules. The possibility has to be considered that overexpression of the fusion protein is not reflecting the native distribution. However, the fact that the bacterially expressed protein binds microtubules in vitro supports the idea that AtMAP70-5 is a bona fide microtubule-associated protein.

Our observations on the overexpression of AtMAP70-5 show similarities to those obtained for the microtubule-associated protein WAVE-DAMPENED2 (WVD2) (Perrin et al., 2007; Yuen et al., 2003). For example, AtMAP70-5 is the only member of the AtMAP70 family to contain the KLEEK motif found in WVD2 and WVD2-like (WDL) proteins (Yuen et al., 2003). The 35S-driven overexpression of WVD2

perturbs anisotropic cell expansion, resulting in concomitantly stockier plants that have right-twisting growth in both roots and hypocotyls. Until now, WVD2 appears to have been the only endogenous plant MAP that induces these effects when overexpressed and so it is interesting that overexpression of AtMAP70-5 also induces this stunted and right-twisting phenotype. AtMAP70-5 and WVD2 are also similar in their response to microtubule-directed drugs. In these AtMAP70-5 overexpressing plants (not shown), as in WVD2-overexpressing plants, the anti-MT herbicide Propyzamide enhances the growth defects seen in roots. By contrast, microtubule-directed drugs induce left-handed growth in wild-type plants as well as in the right-handed mutants *spr1* and *spr2* (also known as *tor1*) (Furutani et al., 2000).

Decreasing the expression of AtMAP70-5 produces stunted inflorescence stems with decreased diameter. The reduction in stem length is likely to be due to a reduction in cell elongation since epidermal and cortical cells of stems are significantly shorter than those of the wild type. It would, therefore, seem that both increases and decreases in the levels of AtMAP70-5 result in a reduced inflorescence stem length although different mechanisms appear to be involved in these size reductions. Overexpression causes a skewing of epidermal cell files, and together with the observed cell swelling, this may account for the decreased stem length. By contrast, RNAi plants show no such twisting, nor do they swell, suggesting that a reduced amount of AtMAP70-5 limits anisotropic cell expansion.

Microtubule stability and plant growth

Several independent observations have indicated that the overall growth pattern of the plant – twisted or straight – is affected by factors that alter microtubule dynamics. For example, destabilization of the cortical microtubule array seems to lead to left-handed helical growth. This was seen in experiments where wild-type plants were grown on low amounts of microtubule drugs (Nakamura et al., 2004). This was also seen in the *mor1* mutant of the XMAP215/MOR1 microtubule-associated protein (Twell et al., 2002) and in the *lefty* mutant background (Thitamadee et al., 2002). By contrast, right-handed helical growth may, at least in some cases, result from stabilization of microtubules. Analyses of microtubule dynamics in plants that expressed an N-terminally modified tubulin (His-TUA6) showed that right-handed helical growth correlates with reduced microtubule dynamicity and higher rate of microtubule rescue after catastrophe (Abe and Hashimoto, 2005). Right-handed growth in transgenic plants expressing mouse MAP4 (coupled to GFP) or overexpressing the plant-specific MAP WVD2 may arise from increased microtubule bundling and the concomitant increase in microtubule stability (Hashimoto, 2002; Perrin et al., 2007). The results of our experiments on the effect of AtMAP70-5 on tubulin polymerization in vitro, which show a shift towards increased microtubule lengths, are consistent with the idea that increased microtubule stability favours right-twisting organ growth.

There are at least two general ways that perturbations of the microtubular cytoskeleton could affect organ anisotropy and twisting. First, files of cells are generated by formative/longitudinal divisions of founder cells in the apical meristem and these so-called T-divisions have been shown to arise around the meristematic growth axis on a helix (Baum and Rost, 1996). Overexpression could affect the three-dimensional patterning of these key divisions. Or, secondly, the overexpression phenotype could be due to a defect of cell expansion rather than proliferation. Consistent with this, epidermal cells in the expansion zone of AtMAP70-5 overexpressors are shorter and have a swollen appearance. Disturbance of anisotropic cell expansion would account for the stunted phenotype but it is not yet known how this translates into helical growth. However, as discussed above, there is emerging evidence that twisted growth is correlated with changes in microtubule dynamics (Abe and Hashimoto, 2005; Sedbrook et al., 2004). In plants, microtubule nucleation and organization are separate processes. After polymerization at dispersed nucleation sites microtubules move across the plasma membrane by a modified form of treadmilling in which microtubules grow more rapidly at the plus end than they shrink at the minus end (Shaw et al., 2003). Changes in the dynamicity of microtubules are therefore likely to affect the rate at which microtubules move. This would have consequences both for the collision rate and for the stability of the newly formed co-linear groups (Shaw et al., 2003; Dixit et al., 2006; Chan et al., 2007). Furthermore, within such groups, microtubules can be cross-bridged by MAP65 (Chan et al., 1999; Mao et al., 2006; Smertenko et al., 2004) so that it is possible that by increasing the stability of cortical microtubules, AtMAP70-5 could be increasing the likelihood that they become cross-bridged and decorated by other MAPs, thereby affecting the structure and dynamics of the microtubule array as a global structure.

In conclusion, the present observations support the idea that changes in the stability of microtubules correlate with changes in anisotropic cell expansion and the direction of organ growth.

Materials and Methods

Microtubule co-sedimentation assay

6XHis:AtMAP70-1 (At1g68060) and 6XHis:AtMAP70-5 (At4g17220) proteins were expressed in *E. coli* [RosettaTM (DE3) pLysS, Novagen, San Diego, USA], purified on a TALON metal affinity column (Clontech, Mountain View, USA) and stored in liquid nitrogen until the assay. Microtubules were pre-assembled by dissolving 1 mg tubulin (Cytoskeleton Inc., Denver, USA) in microtubule stabilising PME buffer (50 mM Pipes pH 6.9, 5 mM EGTA, 5 mM $MgSO_4$) and polymerising in the presence of 10 μM Taxol (Paxitaxel, Sigma, Poole, UK) for 30 minutes at 37°C. 10–50 μg of purified MAP70 protein was incubated with pre-assembled microtubules for 45 minutes at 4°C and centrifuged (Beckman, sw 50 rotor) through a 40% (w/v) sucrose cushion at 65,000 ***g***, for 30 minutes at 4°C. Supernatant and pellet were mixed with SDS-PAGE loading buffer, boiled for 5 minutes and analysed by SDS-PAGE (Sambrook et al., 1989).

Microtubule assembly assay

Microtubules were assembled using fluorescein-conjugated tubulin (Cytoskeleton Inc., Denver, USA) for 1 hour at 37°C in PME buffer containing 5% DMSO and 1 mM GTP. First the critical concentration of tubulin for microtubule self-assembly was determined as 0.5-0.6 μg/ml. Microtubules were assembled in the presence or absence of AtMAP70-5 in a range of concentrations (1-10 μg/ml). To study the effect of AtMAP70-5 on the pre-assembled microtubules, 1 μl of AtMAP70-5 was added to 9 μl of pre-assembled microtubules to a final concentration of 10 μg/ml and incubated at 37°C for 30 minutes. The same amount of PME buffer was added as a control. The microtubules were fixed with glutaraldehyde [1% (v/v) final concentration] and images were captured digitally and processed using Adobe Photoshop and ImageJ software. More than 600 microtubules were measured for each treatment.

Cell suspensions, transformation and imaging

Cell suspension cultures of *Arabidopsis thaliana* L (Heynh.) ecotype Columbia 0 (Mathur et al., 1998) and tobacco (*Nicotiana tabacum* L) Bright Yellow-2 (BY-2) (Nagata et al., 1992) were grown and transformed with *35S::GFP-AtMAP70-5* (pGWB6 vector with an N-terminal GFP tag; Invitrogen, Paisley, UK) as described by Korolev et al. (Korolev et al., 2005). Bright-field images were captured using a Nikon Eclipse 800 microscope equipped with a Pixera Pro ES600 digital camera

(Nikon, Japan). Expression of GFP fusion protein was observed using confocal laser scanning microscopy (Leica DM IRB, SP2). The percentage of transformed (i.e. fluorescent) multipolar cells was determined in BY-2 cultures expressing GFP-TUA6 and GFP-MAP70 and compared to untransformed cultures. At least 1000 cells were counted per sample.

Plant growth, transformation and analysis

Seeds of *Arabidopsis thaliana* (L. Heynh.) ecotype Columbia 0 plants were surface-sterilised in 5% (v/v) bleach for 5 minutes and rinsed 3× 5 minutes in sterile water. Plants were grown in a glasshouse and transformed with *35S::AtMAP70-5*, *35S::GFP-AtMAP70-5* or *35S:AtMAP70-5* RNAi vectors by floral dipping (Clough and Bent, 1998) using the hypervirulent *Agrobacterium tumefaciens* strain LBA4004.pBBR1MCSvirGN54D. The entire coding sequence of *AtMAP70-5* was inserted into both pGWB2 (without GFP tag) and pGWB6 (with N-terminal GFP tag) vectors, Invitrogen, Paisley, UK) and into the RNAi (pFGC5941 dsRNA) constructs (kindly provided by Matt Tomlinson, University of East Anglia, Norwich) .

T1 transformants were selected on agar medium [0.44% (w/v) Murashige and Skoog's powdered medium, 1.5% (w/v) agar, 0.8% (w/v) sucrose; Sigma] containing 100 μg/ml kanamycin sulphate (for AtMAP70-5 and GFP-AtMAP70-5) or by three rounds of spraying of soil-grown plants with BASTA (for AtMAP70-5 RNAi).

To identify the root phenotype, T2 plants were grown vertically on antibiotic-free Phytagel medium [0.44% (w/v) Murashige and Skoog's powdered medium, 0.5% (w/v) Phytagel and 0.8% (w/v) sucrose; Sigma] at 25°C. One-week-old seedlings were transferred to soil and grown in the glasshouse. Stems of the 6-week-old plants were sampled for RNA extraction (see next section) and for analysis of cell shape. The middle third of the stem was cut in 0.5-1 cm fragments and fixed in 4% (w/v) formaldehyde in 50 mM phosphate buffer (pH 7) at 4°C overnight. Samples were washed with 50 mM phosphate buffer and dehydrated in the sequence: 70% ethanol (2 hours), 100% ethanol (overnight), 70% ethanol (2 hours), 20% glycerol/35% ethanol (6 hours), 40% glycerol (overnight). Stem sections were stained with Toluidine Blue [0.001% (v/v) for 20 minutes] or with propidium iodide (10 μg/ml for 5 minutes) in 40% glycerol.

RNA extraction and RT-PCR

RNA was isolated from seedlings (3 days after germination) or from inflorescence stems (upper third) using the RNease Plant Mini kit (Qiagen, Crawley, UK). Reverse transcription (RT) was performed using a SuperScript RT kit (Invitrogen, Paisley, UK). The polymerase chain reaction (PCR) was performed using *AtMAP70* gene-specific primers. RT-PCR for the housekeeping *ATP1* (mitochondrial ATP synthase alpha chain) gene was used as an internal control.

We thank Georgios Kitsios (JIC, Norwich) for GFP-TUA6 BY-2 line and Matt Tomlinson (UEA, Norwich) for pFGC5941 dsRNA vector; Jordi Chan and Grant Calder for advice. This work was financially supported by the BBSRC.

References

Abe, T. and Hashimoto, T. (2005). Altered microtubule dynamics by expression of modified alpha-tubulin protein causes right-handed helical growth in transgenic *Arabidopsis* plants. *Plant J.* **43**, 191-204.

Abe, T., Thitamadee, S. and Hashimoto, T. (2004). Microtubule defects and cell morphogenesis in the lefty1lefty2 tubulin mutant of *Arabidopsis thaliana*. *Plant Cell Physiol.* **45**, 211-220.

Baum, S. F. and Rost, T. L. (1996). Root apical organization in *Arabidopsis thaliana*. 1. Root cap and protoderm. *Protoplasma* **192**, 178-188.

Buschmann, H., Fabri, C. O., Hauptmann, M., Hutzler, P., Laux, T., Lloyd, C. W. and Schaffner, A. R. (2004). Helical growth of the *Arabidopsis* mutant tortifolia1 reveals a plant-specific microtubule-associated protein. *Curr. Biol.* **14**, 1515-1521.

Buschmann, H., Chan, J., Sanchez-Pulido, L., Andrade-Navarro, M. A., Doonan, J. H. and Lloyd, C. W. (2006). Microtubule-associated AIR9 recognizes the cortical division site at preprophase and cell-plate insertion. *Curr. Biol.* **16**, 1938-1943.

Chan, J., Rutten, T. and Lloyd, C. (1996). Isolation of microtubule-associated proteins from carrot cytoskeletons: a 120 kDa MAP decorates all four microtubule arrays and the nucleus. *Plant J.* **10**, 251-259.

Chan, J., Jensen, C. G., Jensen, L. C. W., Bush, M. and Lloyd, C. W. (1999). The 65-kDa carrot microtubule-associated protein forms regularly arranged filamentous cross-bridges between microtubules. *Proc. Natl. Acad. Sci. USA* **96**, 14931-14936.

Chan, J., Calder, G., Fox, S. and Lloyd, C. (2007). Cortical microtubule arrays undergo rotary movements in *Arabidopsis* hypocotyl epidermal cells. *Nat. Cell Biol.* **9**, 171-175.

Clough, S. J. and Bent, A. F. (1998). Floral dip: a simplified method for *Agrobacterium*-mediated transformation of *Arabidopsis thaliana*. *Plant J.* **16**, 735-743.

Dixit, R. and Cyr, R. (2004). Encounters between dynamic cortical microtubules promote ordering of the cortical array through angle-dependent modifications of microtubule behavior. *Plant Cell* **16**, 3274-3284.

Dixit, R., Chang, E. and Cyr, R. (2006). Establishment of polarity during organization of the acentrosomal plant cortical microtubule array. *Mol. Biol. Cell* **17**, 1298-1305.

Ehrhardt, D. W. and Shaw, S. L. (2006). Microtubule dynamics and organization in the plant cortical array. *Annu. Rev. Plant Biol.* **57**, 859-875.

Furutani, I., Watanabe, Y., Prieto, R., Masukawa, M., Suzuki, K., Naoi, K., Thitamadee, S., Shikanai, T. and Hashimoto, T. (2000). The SPIRAL genes are required for directional control of cell elongation in *Arabidopsis thaliana*. *Development* **127**, 4443-4453.

Hashimoto, T. (2002). Molecular genetic analysis of left-right handedness in plants. *Philos. Trans. R. Soc. Lond. B Biol. Sci.* **357**, 799-808.

Korolev, A. V., Chan, J., Naldrett, M. J., Doonan, J. H. and Lloyd, C. W. (2005). Identification of a novel family of 70 kDa microtubule-associated proteins in *Arabidopsis* cells. *Plant J.* **42**, 547-555.

Lupas, A. (1996). Coiled coils: new structures and new functions. *Trends Biochem. Sci.* **21**, 375-382.

Mao, G. J., Buschmann, H., Doonan, J. H. and Lloyd, C. W. (2006). The role of MAP65-1 in microtubule bundling during *Zinnia* tracheary element formation. *J. Cell Sci.* **119**, 753-758.

Mao, T. L., Jin, L. F., Li, H., Liu, B. and Yuan, M. (2005). Two microtubule-associated proteins of the *Arabidopsis* MAP65 family function differently on microtubules. *Plant Physiol.* **138**, 654-662.

Mathur, J., Szabados, L., Schaefer, S., Grunenberg, B., Lossow, A., Jonas-Straube, E., Schell, J., Koncz, C. and Koncz-Kalman, Z. (1998). Gene identification with sequenced T-DNA tags generated by transformation of *Arabidopsis* cell suspension. *Plant J.* **13**, 707-716.

Nagata, T., Nemoto, Y. and Hasezawa, S. (1992). Tobacco by-2 cell-line as the hela-cell in the cell biology of higher-plants. *Int. Rev. Cytol.* **132**, 1-30.

Nakajima, K., Furutani, I., Tachimoto, H., Matsubara, H. and Hashimoto, T. (2004). SPIRAL1 encodes a plant-specific microtubule-localized protein required for directional control of rapidly expanding *Arabidopsis* cells. *Plant Cell* **16**, 1178-1190.

Nakamura, M., Naoi, K., Shoji, T. and Hashimoto, T. (2004). Low concentrations of propyzamide and oryzalin alter microtubule dynamics in *Arabidopsis* epidermal cells. *Plant Cell Physiol.* **45**, 1330-1334.

Paredez, A., Somerville, C. and Ehrhardt, D. (2006). Visualization of cellulose synthase demonstrates functional association with microtubules. *Science* **312**, 1491-1495.

Perrin, R. M., Wang, Y., Yuen, C. Y. L., Will, J. and Masson, P. (2007). WVD2 is a novel microtubule-associated protein in *Arabidopsis thaliana*. *Plant J.* **49**, 961-1129.

Sambrook, J., Fritsch, E. F. and Maniatis, T. (1989). *Molecular Cloning: A Laboratory Manual*. Cold Spring Harbor, NY: Cold Spring Harbor Laboratory Press.

Sedbrook, J. C., Ehrhardt, D. W., Fisher, S. E., Scheible, W. R. and Somerville, C. R. (2004). The *Arabidopsis* SKU6/SPIRAL1 gene encodes a plus end-localized microtubule-interacting protein involved in directional cell expansion. *Plant Cell* **16**, 1506-1520.

Shaw, S. L., Kamyar, R. and Ehrhardt, D. W. (2003). Sustained microtubule treadmilling in *Arabidopsis* cortical arrays. *Science* **300**, 1715-1718.

Smertenko, A., Saleh, N., Igarashi, H., Mori, H., Hauser-Hahn, I., Jiang, C. J., Sonobe, S., Lloyd, C. W. and Hussey, P. J. (2000). A new class of microtubule-associated proteins in plants. *Nat. Cell Biol.* **2**, 750-753.

Smertenko, A. P., Chang, H. Y., Wagner, V., Kaloriti, D., Fenyk, S., Sonobe, S., Lloyd, C., Hauser, M. T. and Hussey, P. J. (2004). The *Arabidopsis* microtubule-associated protein AtMAP65-1: Molecular analysis of its microtubule bundling activity. *Plant Cell* **16**, 2035-2047.

Thitamadee, S., Tuchihara, K. and Hashimoto, T. (2002). Microtubule basis for left-handed helical growth in *Arabidopsis*. *Nature* **417**, 193-196.

Torres-Ruiz, R. A. and Jurgens, G. (1994). Mutations in the FASS gene uncouple pattern formation and morphogenesis in *Arabidopsis* development. *Development* **120**, 2967-2978.

Traas, J., Bellini, C., Nacry, P., Kronenberger, J., Bouchez, D., and Caboche, M. (1995). Normal differentiation patterns in plants lacking microtubular preprophase bands. *Nature* **375**, 676-677.

Twell, D., Park, S. K., Hawkins, T. J., Schubert, D., Schmidt, R., Smertenko, A. and Hussey, P. J. (2002). MOR1/GEM1 has an essential role in the plant-specific cytokinetic phragmoplast. *Nat. Cell Biol.* **4**, 711-714.

Van Damme, D., Bouget, F. Y., van Poucke, K., Inze, D. and Geelen, D. (2004a). Molecular dissection of plant cytokinesis and phragmoplast structure: a survey of GFP-tagged proteins. *Plant J.* **40**, 386-398.

Van Damme, D., Van Poucke, K., Boutant, E., Ritzenthaler, C., Inze, D. and Geelen, D. (2004b). In vivo dynamics and differential microtubule-binding activities of MAP65 proteins. *Plant Physiol.* **136**, 3956-3967.

Van Damme, D., Coutuer, S., De Rycke, R., Bouget, F.-Y., Inzé, D. and Geelen, D. (2006). Somatic cytokinesis and pollen maturation in *Arabidopsis* depend on TPLATE, which has domains similar to coat proteins. *Plant Cell* **18**, 3502-3518.

Whittington, A. T., Vugrek, O., Wei, K. J., Hasenbein, N. G., Sugimoto, K., Rashbrooke, M. C. and Wasteneys, G. O. (2001). MOR1 is essential for organizing cortical microtubules in plants. *Nature* **411**, 610-613.

Yuen, C. Y., Pearlman, R. S., Silo-Suh, L., Hilson, P., Carroll, K. L. and Masson, P. H. (2003). WVD2 and WDL1 modulate helical organ growth and anisotropic cell expansion in *Arabidopsis*. *Plant Physiol.* **131**, 493-506.